

Using Parasitic Elements for Implementing the Rotating Antenna for MIMO Receivers

Robert Bains and Ralf R. Müller, *Senior Member, IEEE*

Abstract—We consider a new concept of a Multiple-Input-Multiple-Output (MIMO) receiver which uses one active receiving antenna and multiple parasitic elements. The parasitic elements give the possibility of creating a directive antenna beam which is rotated 360 degrees around within the duration of a symbol period. The received signal which is accessed at the antenna connector of the active antenna is expanded in frequency bandwidth compared to the transmitted signal. We show that each sub-band of the received signal consists of linearly independent combinations of the transmitted signals, and thus we have obtained a MIMO receiver. We give a few examples on how to implement this receiver and also explain the effects of sampling the wave-field at discrete angular directions.

Index Terms—MIMO systems, transmission technology, transceiver design.

I. INTRODUCTION

MULTIPLE-INPUT-MULTIPLE-OUTPUT (MIMO) is a technology that promises much higher bit rates than previously achieved with Single-Input-Single-Output (SISO). It has been shown that capacity scales linearly with the minimum number of receiver and transmitter antennas [1], [2] when the channel coefficients are identically independent distributed (i.i.d) complex Gaussian entries. Size restrictions of the mobile terminal however limits the number of antennas that might be included. Too small separation of the antennas will most likely result in a high spatial correlation of the signals and therefore give lower capacity compared to the i.i.d case [3], [4]. When many antennas are packed into a small volume, other effects such as mutual coupling will become dominant. Mutual coupling is shown to decorrelate the signals at the antenna connectors in some cases [5]–[8], and therefore may give a higher capacity than first expected. An additional effect of mutual coupling is that it changes the antenna impedance, which may lead to impedance mismatch if no matching network is used. Several papers have considered this effect [9]–[13]. Impedance mismatch is especially deleterious when the dominant signal impairment is receiver/amplifier noise. Impedance mismatch yields lower received signal power and therefore reduces receiver signal-to-noise ratio (SNR). Instead of focusing on mutual coupling some authors have described the number of degrees of freedom of the electromagnetic field. Reference [14], [15] have expressed the degrees of freedom by the wavevector-aperture product, $\mathcal{A}|\Omega|$. The

Manuscript received October 10, 2006; revised March 20, 2007 and May 29, 2007; accepted August 1, 2007. The associate editor coordinating the review of this paper and approving it for publication was A. Molisch.

The authors are with the Faculty of Information Technology, Norwegian University of Science and Technology, Trondheim, Norway (e-mail: rains@iet.ntnu.no).

Digital Object Identifier 10.1109/T-WC.2008.060808

symbol \mathcal{A} represents the effective aperture which relates to the geometrical size of the transmitter/receiver, and $|\Omega|$ is the angular spread of the scatterers. Reference [16] relates in a different way the effective number of degrees of freedom of the field on a given observation curve, surface or volume to the number of (spatial) Nyquist intervals the observation curve encompasses. The number of singular values of the electromagnetic field and their relative strengths then gives the possibilities for finding capacity expressions. However these capacity expressions are only approximations. Different results may be obtained when the measurement devices (antennas) are included. The antennas themselves, simply by being conductive material, affect the electromagnetic field.

This paper explores another concept for a MIMO receiver which is quite different from previous research on MIMO. Instead of sampling values of the electromagnetic field with antennas at discrete spatial points, we propose to over-sample values of the field at the same physical location. We suggest a time-variant receiver which makes sure that the antenna pattern is time varying during a symbol period. It will be shown that spatial multiplexing can be converted into frequency multiplexing. As a result of this, different sub-channels are created in the frequency domain. These sub-channels have the same effect as multiple receive antennas in traditional MIMO systems. Except for [17] we have not seen this concept been suggested before. An independent parallel work to ours [18], [19] has considered a similar concept. They have, as far as the authors know, only focused on the transmitter issues, whereas this work only studies the receiver. Our concept cannot be employed directly in a transmitter for reasons that will be explained in this paper.

The paper is organized as follows: Section II presents the general concept of the proposed receiver, Section III deals with the practical implementation of the receiver, Section IV presents some thoughts on signal power, noise and adjacent channel interference, Section V discusses sampling issues, Section VI addresses the dependence of performance on scattering richness, Section VII gives the conclusion, and Section VIII mentions open problems that are yet to be solved.

II. A ROTATING RECEIVER ANTENNA

This section aims to describe the concept without considering its physical implementability. This is left for the succeeding sections, which deal with practical implementations.

Consider a directive receiver antenna that has the ability to rotate 360 degrees around periodically. Assume the rotation speed to be at least equal to one rotation per symbol period. The antenna would then, during the symbol period, pick up

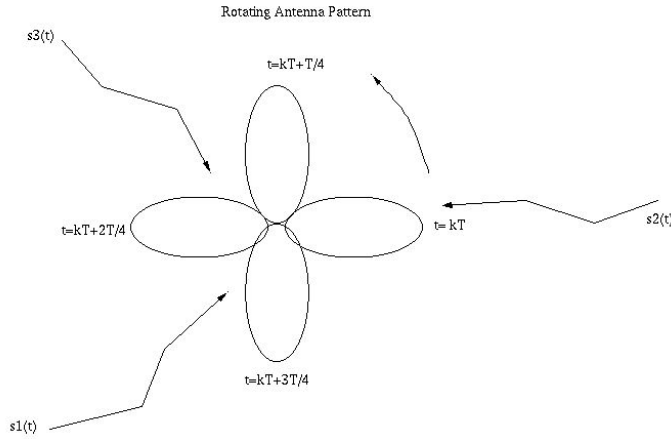


Fig. 1. Rotating antenna pattern. The direction of the antenna beam is shown for $t = kT$, $kT + T/4$, $kT + 2T/4$, $kT + 3T/4$. For each of the antenna beam directions the incoming signals $s_1(t)$, $s_2(t)$, $s_3(t)$ are weighted in a different way.

different linear combinations of the signals arriving at various azimuthal angles. For simplicity we assume a two-dimensional (2D) model, with all signals arriving from the azimuth-plane. We consider P signals arriving towards the antenna at different angles. Let $s_p(t)$ be the signal coming from angle ϕ_p . The signal $s_p(t)$ is weighted by the antenna according to the antenna pattern function $a(\phi_p)$. Consider now that the antenna rotates with an angular speed ω rad/s, thus $r(t)$ which is the received signal can then be described by:

$$r(t) = \sum_{p=1}^P a(\omega t + \phi_p) s_p(t) \quad (1)$$

The antenna pattern function $a(\omega t + \phi)$ has now a time-dependency because of the rotation. Fig. 1 gives a pictorial description of the antenna rotation.

We need a certain requirement on the rotation speed

$$\frac{1}{T} \leq \frac{\omega}{2\pi} \ll f_c \quad (2)$$

where T is the symbol time and f_c is the carrier frequency. This requirement must hold in order to avoid aliasing. The necessity of (2) will be explained later in this section. Since the antenna pattern function is a periodic function, we note that it can be Fourier expanded

$$a(\omega t) = \sum_{l=-L}^{+L} a_l e^{jl\omega t} \quad (3)$$

where we have assumed the antenna pattern function to be bandlimited, with a total of $2L + 1$ frequency components. The l -th frequency component is given by a_l . There is one component a_0 at the fundamental frequency and $2L$ harmonics. By inserting (3) into (1) we obtain:

$$r(t) = \sum_{l=-L}^{+L} e^{jl\omega t} a_l \underbrace{\sum_{p=1}^P e^{jl\phi_p} s_p(t)}_{r_l(t)} \quad (4)$$

From this expression we see that the physical rotation of the antenna results in frequency-shifts of the received signal. If the

signal $s_p(t)$ is centered around carrier frequency ω_c then the multiplication with $e^{jl\omega t}$ results in the signal being frequency-shifted to $\omega_c + l\omega$. Each frequency-shift corresponds to a sub-band. Fig. 2 shows how the signal bandwidth is expanded. Going back to inequality (2), we see that the lower bound needs to be fulfilled in order to avoid spectral aliasing between the subbands. The rotation speed ω can be exactly equal to $\frac{2\pi}{T}$ if the signals $s_p(t)$, $p = 1 \dots P$ have a bandwidth $\leq \frac{1}{T}$. In many cases the bandwidth is larger and therefore a larger rotation speed is needed. The sub-band components can be separated by means of band-pass filtering. We can express the sub-band components in vector notation.

$$\begin{aligned} \underbrace{\begin{bmatrix} r_{-L}(t) \\ \vdots \\ r_{+L}(t) \end{bmatrix}}_{\mathbf{r}(t)} &= \underbrace{\begin{bmatrix} a_{-L} & 0 & 0 \\ 0 & \ddots & 0 \\ 0 & 0 & a_{+L} \end{bmatrix}}_{\mathbf{A}} \\ &\cdot \underbrace{\begin{bmatrix} e^{-jL\phi_1} & \dots & e^{-jL\phi_P} \\ \vdots & \ddots & \vdots \\ e^{+jL\phi_1} & \dots & e^{+jL\phi_P} \end{bmatrix}}_{\mathbf{V}} \underbrace{\begin{bmatrix} s_1(t) \\ \vdots \\ s_P(t) \end{bmatrix}}_{\mathbf{s}(t)} \end{aligned} \quad (5)$$

where $r_{-l}(t)$ is the sub-band around center frequency $f_c - \frac{l\omega}{2\pi}$. The matrix \mathbf{A} consists of the Fourier components of the antenna pattern. The components of \mathbf{A} also indicate the strengths of each sub-band signal. The matrix \mathbf{V} is an operator that makes linear combinations of the incoming signals, given by $\mathbf{s}(t)$, and outputs these linear combinations in each of the $2L + 1$ sub-bands. Each sub-band can be interpreted as having the same effect as a separate antenna in regular MIMO-systems. This holds because in regular MIMO each antenna would pick up different linear combinations of the incoming waves. To increase the spatial multiplexing gain we should opt for an antenna pattern with as many Fourier-components as possible. If the scattering is sufficiently rich, then the number of Fourier-components would be the limiting factor of our system. There are two ways of obtaining an antenna pattern with a high number of Fourier components. We could try to create antenna patterns with one narrow beam. The other approach is to create shapes different from the previous one that have a high variation in the azimuth plane. We have taken the former approach in this paper.

Since this antenna system expands the frequency bandwidth it can obviously not be used as a transmitter. The transmitted signal would then consist of an expanded bandwidth and hence violate the spectrum regulations. So as a transmitter it would need to use a non-rotating antenna pattern. But as the authors see it, the down-link for a mobile-terminal is more rate critical than the up-link. It is important to note that the bandwidth expansion is just seen by the rotating receiver antenna. The antenna rotation modulates the received signal onto different sub-bands. If the other users do not have a rotating antenna, they will not see an expanded bandwidth.

There are some references [20] that have suggested using oscillating antenna patterns for time-diversity. They let the antenna pattern fluctuate around a main beam angle and hence their scheme differs from ours. Their goals and our goals are

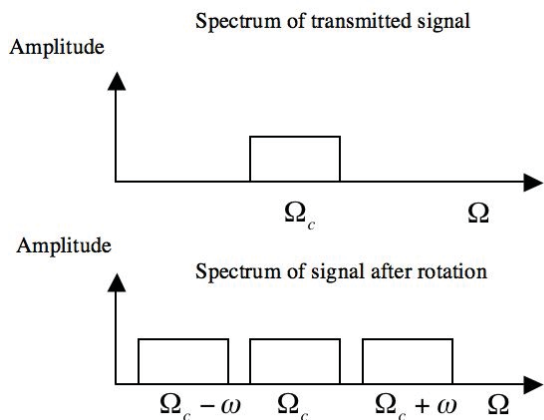


Fig. 2. The spectrum of a signal transmitted at carrier frequency Ω_c is shown. Assuming an antenna rotation of ω rad/s and an antenna pattern with three frequency components the signal gets expanded in frequency, with spectral copies centered at $\Omega_c - \omega$ and $\Omega_c + \omega$.

also different, since we are interested in spatial multiplexing gain, whereas they are interested in diversity.

III. PRACTICAL IMPLEMENTATION: SAMPLED ROTATING ANTENNA

The implementation of the physically rotating antenna is not practical. However there is a possibility of using switched parasitic elements to form a directive antenna beam [21]–[25]. We hereby call the practical implementation of the rotating antenna a sampled rotating antenna. Switched parasitic elements have been employed before but for the purpose of increased diversity gain. Diversity gain does not require fast switching and bandwidth expansion as the proposed scheme does. Three different practical ways are proposed to implement the rotating antenna. Section III-A deals with parasitic elements that are either short-circuited or open-circuited. Section III-B proposes the use of reactive loads within the parasitic elements or alternatively by the use of parasitic elements with variable lengths. Section III-C addresses the impact of mutual coupling on the obtainable antenna patterns.

A. Short circuited/Open circuited parasitic elements

Parasitic elements can be used to enable virtual rotation of the antenna. As an example, consider a half wavelength dipole as a receiver antenna. Then assume that a similar dipole antenna (parasitic) is placed in close vicinity to the receiver antenna. If the parasitic element is short-circuited in the middle, the antenna pattern becomes somewhat directive. The obtained antenna pattern when a parasitic element is placed at distance $\lambda/64$ from the receiver antenna, where λ denotes the carrier wavelength, is shown in Fig. 3. All the antenna patterns in this paper were found by using a commercial software [26]. This close distance is however not practical, since it leads to an antenna impedance which is far from the standard 50 ohm impedance used in the industry. Therefore to avoid matching circuits that introduce power-loss, a somewhat larger distance between the elements must be used. If we place

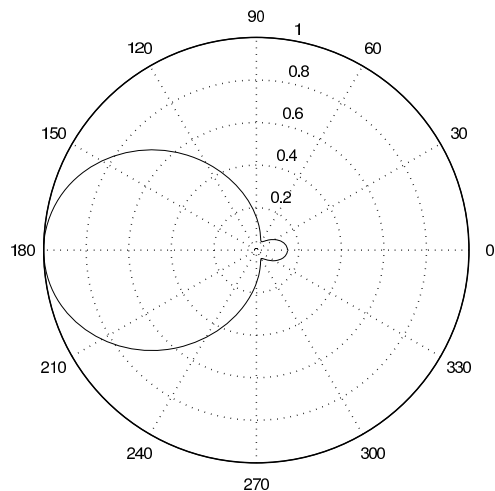


Fig. 3. An antenna pattern obtained by short-circuiting one parasitic element. The parasitic element is placed at distance $\lambda/64$ to the active element. The antenna pattern is normalized and drawn in linear scale, and is found by using an antenna simulation software [26].

an electronic switch within the parasitic element we have the possibility to either short-circuit or open-circuit the parasitic element. When the parasitic element is open-circuited, it will be equivalent to two dipoles of lengths $\lambda/4$. A dipole of length $\lambda/4$ is not resonant with the electromagnetic field, and it will therefore hardly alter the antenna pattern of the active receiving antenna. From this a simple scheme can be found to achieve the rotation of a directive antenna beam. Consider placing a number of parasitic elements on a circle around the active receiving antenna. The parasitic elements can be placed at the following angles

$$\phi_i = \frac{2\pi i}{2L+1} \quad i = -L \dots L \quad (6)$$

By letting the parasitic elements be short-circuited in a TDMA-like fashion we are able to rotate a directive antenna beam 360 degrees around by discrete steps. The parasitic element will act as a reflector when it is short-circuited. This means that the beam will point into the opposite direction of the parasitic element. Note that the number of parasitic elements is chosen to be $2L+1$, i.e. equal to the number of frequency components of the antenna pattern. This number of samples per rotation is sufficient according to the sampling theorem. This can be understood from the fact that $a(\omega t)$ is band-limited with bandwidth $(2L+1)\omega$.

To demonstrate the achievable spatial multiplexing gain with the proposed receiver, we performed simulations of mutual information. We assumed perfect channel knowledge at the receiver side. The simulations were performed for different distances between the parasitic elements and the active receiving dipole. The parasitic elements were placed on a circle around the active receiving antenna. To study solely the effect of the receiver on mutual information, we chose the transmitters to be a linear array of 20 elements. We chose to model the channel by ray tracing plane waves scattered at 120 random positions. The relatively high number of scatterers was chosen in order to avoid statistical dependencies in the channel matrix [27]. The linear scaling of mutual information with the number of degrees of freedom is best observed at high SNR.

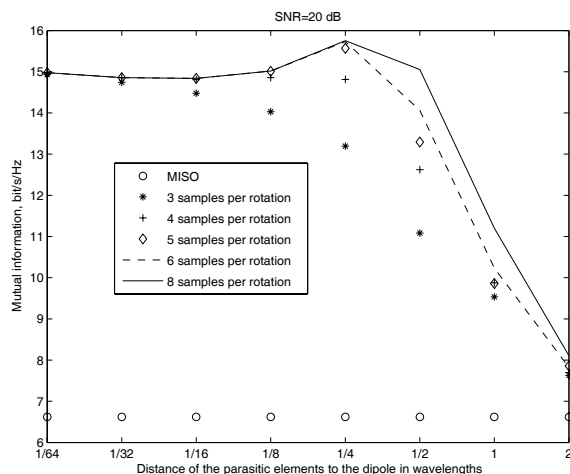


Fig. 4. Mutual information as a function of the distance between the parasitic elements and the active receiver. The number of parasitic elements corresponds to the number of samples per rotation.

Therefore we chose the noise to be circularly complex additive white Gaussian noise (AWGN) 20 dB below the received signal power. Note that the noise is assumed predominantly to be channel noise, and therefore the antenna efficiency is not considered to be important. A low antenna efficiency would mean that less power is extracted from the incoming waves. But since the same would happen to the channel noise, the receiver SNR would not change significantly. In Section IV the appropriate normalization and scaling of the noise will be considered. This scaling is also taken into account when calculating the results for the present section.

Fig. 4 shows ergodic mutual information versus distance to the active receiver for various numbers of parasitic elements. Since only one parasitic element is short-circuited at a time, the number of parasitic elements is equivalent to the number of directions the antenna listens to. This means that the number of parasitic elements is equal to the number of samples of the antenna pattern per rotation. It seems that three samples per rotation are sufficient for small distances. The reason for this is that the antenna pattern consists only of 3 main frequency components for small distances. Therefore according to the sampling theorem it is sufficient to oversample 3-fold. This is confirmed by the fact that 8 samples per rotation does not give a higher mutual information than 3 samples for distances smaller than $\lambda/32$. When the distance is around a quarter wavelength, 3 samples per rotation are not sufficient. For this distance the antenna pattern consists of more than 3 main frequencies, and therefore 3 samples per rotation results in aliasing. For even larger distances between the parasitics and the active antenna the mutual information decays. The reason is that mutual coupling becomes lower for larger distances, and therefore the influence of the parasitic elements on the antenna pattern decays.

Note that short-circuiting more than one parasitic element at a time gives the possibility to create several more antenna patterns. $2L + 1$ parasitic elements could achieve a total of 2^{2L+1} different patterns. However most of these antenna patterns would correspond to significantly different antenna

impedances. This constitutes a severe obstacle to practical implementation. However reference [28] proposed dynamic matching such that multiple different antenna impedances can be coped with. By short-circuiting one parasitic element at a time we avoid the problem of matching several impedances. Since the parasitic elements are placed symmetrically on a circle they will give the same antenna impedance, independent from which of the parasitics that are short-circuited.

In this paper we assume that the electronic switches are ideal with zero switch delay. For low-cost implementation p-type, intrinsic, n-type (p.i.n) diodes might be used. Reference [29] shows that p.i.n diode switches have delays of the order of nano-seconds. During this delay the impedance of the p.i.n diode will change from a high impedance value to a low impedance value or vice versa. Since one parasitic element is going from short-circuit to open-circuit and another parasitic element is going from open-circuit to short-circuit there will be a time interval where both elements are conductive. The received signal during this time interval is hard to predict, and can be considered to be random in nature. Other switches that might be used in the future if their switching time is shortened are Micro-Electro-Mechanical Systems (MEMs) [30] switches.

B. Reactive loading and parasitics with variable lengths

The previous section showed that the maximum number of degrees of freedom obtained was 3 to 4 when using short/open-circuited parasitic elements. In order to be able to achieve even more directive patterns different techniques need to be employed. Reference [31] shows that it is possible to achieve directive patterns by loading the parasitic elements with reactive impedances. The values of the reactive loads are found by maximizing a gain function. However, this gain function has several local maxima. Fig. 5 shows an antenna pattern which is obtained by reactively loading 6 parasitic elements. The parasitic elements are placed at distance $\lambda/8$ to the active antenna. This antenna pattern gives 5 dominant frequency components. This means that 5 degrees of freedom can be used for communication. The switching of the parasitic elements however gets more complicated, since we now have to switch amongst different values of reactive loads. When the antenna rotates it will have the same antenna impedance for each of the directions it listens to. The reason is the same as when short-circuiting one parasitic element at a time. For each direction the antenna listens to the same reactive loads are used. However each parasitic are using different reactive loads for each direction. But since the parasitic elements are placed on a circle around the active antenna, the antenna impedance will be the same from the perspective of the active antenna. As a means of realizing the reactive loading, one can attach transmission lines in the middle of the parasitic elements. The lengths of these transmission lines determine then the reactive value they represent. An even better choice would be to use varactor diodes. Varactor diodes have the ability to attain different reactive values by means of an input control signal. Another work [32] has also used reactive loading of parasitic elements for a MIMO transceiver, however, their motivation was to create orthogonal patterns for two active dipole antennas.

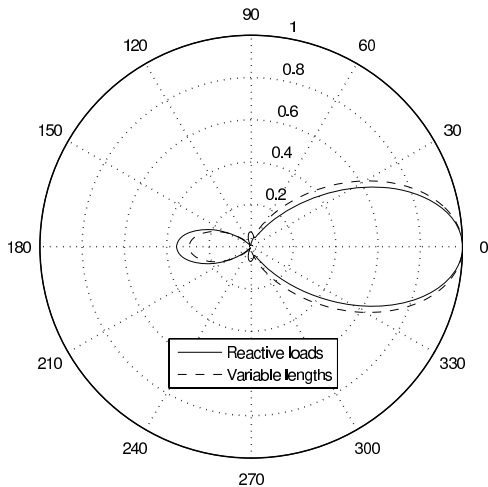


Fig. 5. Antenna patterns obtained respectively by reactively loading 6 parasitic elements (solid line) and employing parasitic elements with variable lengths (dashed line). Distance $\lambda/8$ between the parasitic elements and the active receiver. The antenna patterns are drawn in linear scale. Each of the antenna patterns are normalized independently. The patterns were found by using an antenna simulation software [26].

Another way of realizing directive antenna patterns is by letting the parasitic elements have variable lengths. This can be done by using multiple switches on the parasitic elements. Fig. 5 shows an antenna pattern which is obtained by using variable lengths of the parasitic elements.

We have performed simulations of ergodic mutual information for both reactive loading and parasitic elements with variable lengths. The distance between the parasitic elements and the active receiver was chosen to be $\lambda/8$. This ensures that the total volume of the antenna system is less than $\frac{\lambda^3}{40}$. In order to investigate the broadband properties of mutual information we have performed the simulations for different frequencies. We have considered perfect impedance matching of the active antenna over the entire frequency range. So the broadband property of mutual information does not relate to impedance mismatch, but rather relates to how the antenna pattern changes with frequency. We realize that this assumption may be unrealistic in practice since compact antennas tend to have low antenna efficiency bandwidths [33]. But as an initial stage investigation of the broadband properties we only consider how the antenna pattern changes with frequency. For the simulations, the same channel model is assumed as before, ray tracing with 120 scatterers at random angular directions. Fig. 6 shows that using reactive loads gives a mutual information that is 3.3 times higher than the mutual information obtained by MISO. The antenna patterns were designed for the carrier frequency 2.5 GHz. Mutual information seems to attain approximately the same value over a 100 MHz frequency range when employing reactive loading. Parasitic elements with variable lengths were found to be less robust with respect to frequency variation. After seeing the antenna patterns obtained by reactive loading and parasitic elements with variable lengths, a natural question might be if there is any limit, for a certain volume, on how directive our antenna can become. According to [34] there does not exist any theoretical limit on directivity for a fixed aperture size, but very directive antennas often give unwanted effects

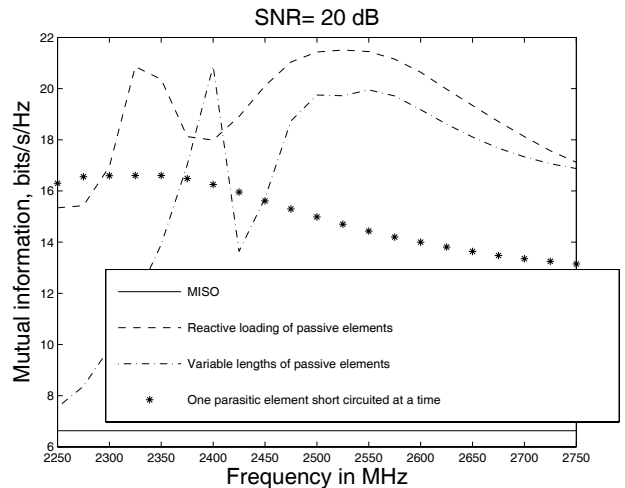


Fig. 6. Mutual information over different frequencies. Distance $\lambda/8$ between the parasitic elements and the active receiver. 6 parasitic elements are used.

such as narrow bandwidth, poor antenna efficiency and low tolerance against production inaccuracies of the antenna. An example of super-directive antennas with parasitic elements is found in [35]. There are some authors that have considered super-directivity in their capacity expressions, e.g [36] gives the possibility of finding capacity when there is a constraint on the maximum super-directivity factor, Q .

When the antenna patterns were calculated it was assumed that the conductance of the wire antennas was infinite. For verification purposes simulations with realistic conductances of the elements were also performed which showed only negligible differences in the antenna patterns.

C. The impact of mutual coupling on the antenna pattern

In this section we want to quantify the impact of mutual coupling on the obtainable antenna patterns. For simplicity we only consider the case when the parasitic elements are either short-circuited or open-circuited. Consider one active element and one parasitic element. Because of reciprocity, the antenna pattern when the antenna is transmitting and receiving will be the same. We can find the antenna pattern when the antenna is transmitting and then argue that the same pattern holds when the antenna system is receiving. Consider that the active antenna is placed at the center of a coordinate system and directed along the z-axis. The electrical far field component at a point in space can be expressed as [37]:

$$E_{\theta} \approx j\eta \frac{i_1 e^{-j\frac{2\pi}{\lambda}r}}{2\pi r} \left[\frac{\cos(\frac{\pi l}{\lambda} \cos(\theta)) - \cos(\frac{\pi l}{\lambda})}{\sin(\theta)} \right] \quad (7)$$

where E_{θ} is one of the three orthogonal components that the electric field can be decomposed into. The two other orthogonal components are equal to zero. It is assumed in the derivation of (7) that the current on the antenna has a sinusoidal distribution, with i_1 being the maximum value of the current on the active antenna. The angle θ is the zenith angle from the positive z-axis, l is the length of the antenna, r is the radius from the origin of the coordinate system to the point in space, η is the intrinsic impedance of the propagation

medium (air) and λ is the carrier-wavelength. We are interested in evaluating the electric field in the azimuth plane which corresponds to $\theta = \frac{\pi}{2}$. We define the antenna pattern in the azimuth plane as:

$$\begin{aligned} a(\phi) &= rE_{\theta,1}(\phi) + rE_{\theta,2}(\phi) \\ &= \frac{j\eta}{2\pi} \left(i_1 + i_2 \cdot e^{j \frac{2\pi}{\lambda} \cdot d \cos(\phi)} \right) \end{aligned} \quad (8)$$

where ϕ is the azimuth angle, $E_{\theta,1}(\phi)$ and $E_{\theta,2}(\phi)$ are the electric field contributions from the active and parasitic antenna respectively, i_1 is the current on the active antenna, i_2 is the current on the parasitic antenna and d is the inter-element distance.

The currents on the antenna elements can be expressed by taking into account the mutual coupling.

$$\begin{aligned} i_1 &= \frac{Z_{11} \cdot V}{Z_{11}(Z_{11} + Z_L) - Z_{12}^2} \\ i_2 &= -\frac{Z_{12}V}{Z_{11}(Z_{11} + Z_L) - Z_{12}^2} = -\frac{Z_{12}}{Z_{11}} \cdot i_1 \end{aligned} \quad (9)$$

where Z_{11} is the self-impedance of the active and parasitic element, Z_{12} is the mutual coupling between the active and parasitic element, Z_L is the termination impedance of the active antenna and V is the voltage source attached to the active antenna. The Fourier components of the antenna pattern can be found by combining (8), (9) and by taking the Fourier transform:

$$\begin{aligned} a_0 &= \frac{j\eta}{2\pi} \left(i_1 + i_2 \cdot J_0\left(\frac{2\pi}{\lambda} \cdot d\right) \right) \\ &= \frac{j\eta \cdot i_1}{2\pi} \cdot \left(1 - \frac{Z_{12}}{Z_{11}} \cdot J_0\left(\frac{2\pi}{\lambda} \cdot d\right) \right) \\ a_l &= -\frac{\eta \cdot i_2}{2\pi} \cdot J_l\left(\frac{2\pi}{\lambda} \cdot d\right) \\ &= \frac{\eta \cdot i_1}{2\pi} \cdot \frac{Z_{12}}{Z_{11}} \cdot J_l\left(\frac{2\pi}{\lambda} \cdot d\right), l = -L \dots L, l \neq 0 \end{aligned} \quad (10)$$

where a_l is the l -th Fourier component and $J_l(\cdot)$ is the Bessel function of the first kind of order l . Higher order Bessel functions are almost zero valued when the argument of the function is small, which means that small inter-element distances, i.e. small arguments of $J_l(\cdot)$, lead to Fourier components with small amplitudes. As a result of this, small inter-element distances generally lead to antenna patterns with 3 main Fourier components. As an example consider an inter-element spacing of $\lambda/64$. According to (10) the antenna pattern consists of 3 Fourier components with equal strengths. By increasing the inter-element distance to $\lambda/4$, we also increase the number of Fourier components of the antenna pattern. This is in agreement with the results of Fig. 4 which shows a peak in mutual information at an inter-element distance of $\lambda/4$. Note that increasing the inter-element distances beyond $\lambda/4$ will not be beneficial since the mutual coupling between the elements becomes smaller. This can also be observed from Fig. 4.

The fact that small inter-element distances give larger mutual-coupling than larger distances, and that the values of the Bessel functions become lower for smaller inter-element distances suggests that there should be an optimum inter-element distance.

IV. SIGNAL POWER, NOISE AND ADJACENT CHANNEL INTERFERENCE

From (5) it is clear that the bandwidth of the received signal becomes wider. Then it becomes natural to consider what happens to the SNR. For that purpose we compare the SNR when the antenna is a conventional non-rotating antenna to a rotating antenna. The signal of interest which is accessed by the conventional and the rotating antenna is denoted by $r_{conv}(t)$ and $r_{rot}(t)$ respectively. We assume that the signal has a bandwidth $\frac{1}{T_s}$. The received energy during the symbol interval T_s is given by:

$$\int_0^{T_s} |r_{conv}(t)|^2 dt = E \quad (11)$$

The noise is assumed to be AWGN with power spectral density (psd) N_0 J/s/Hz. This means that the SNR becomes:

$$\text{SNR}_{conv} = \frac{E}{N_0} \quad (12)$$

In order to benefit from the rotating antenna we would need to over-sample. This means that for each sample the signal is accessed for a shorter time period. When the signal bandwidth is expanded by a factor $2L + 1$ we need a sampling rate of $(2L + 1) \cdot \frac{1}{T_s}$ samples/second. The energy of the signal during sample interval $\frac{T_s}{2L+1}$ becomes:

$$\int_0^{T_s/(2L+1)} |r_{rot}(t)|^2 dt = \frac{E}{2L+1} \quad (13)$$

The bandwidth of the noise becomes $\frac{2L+1}{T_s}$ for the rotating antenna. The noise is however accessed for a smaller time-interval, $\frac{T_s}{2L+1}$. This means that the noise energy during the sampling interval $\frac{T_s}{2L+1}$ becomes N_0 . The effective SNR for the rotating antenna is therefore reduced:

$$\text{SNR}_{rot} = \frac{E}{(2L+1) \cdot N_0} \quad (14)$$

This expression shows that the SNR is decreased by the over-sampling factor. We next search for a rough expression for the mutual information.

First we need to define the received signal:

$$\mathbf{r} = \frac{E}{N_0} \mathbf{A} \mathbf{V} \mathbf{H} \mathbf{x} + \mathbf{n} \quad (15)$$

where A and V are the same matrices as in (5), \mathbf{H} describes the channel from the transmitter antennas to a certain angular direction at the receiver, \mathbf{x} is the transmit signal vector and \mathbf{n} is a zero mean AWGN-vector with unit variance. We have in addition $\mathbb{E}\{\text{tr}(\mathbf{A} \mathbf{V} \mathbf{H} \mathbf{H}^H \mathbf{V}^H \mathbf{A}^H)\} = 1$. The mutual information when the channel is known to the receiver but unknown to the transmitter becomes:

$$\begin{aligned} I(\mathbf{r}; \mathbf{x}) &= \log_2 \left(\mathbf{I} + \frac{E}{N_0} \mathbf{A} \mathbf{V} \mathbf{H} \mathbf{H}^H \mathbf{V}^H \mathbf{A}^H \right) \\ &= \sum_{l=1}^{2L+1} \log_2 \left(1 + \frac{E}{N_0} \sigma_l^2 \right) \end{aligned} \quad (16)$$

where σ_l is l -th singular value of the channel decomposition. By assuming high SNR, an approximate expression for the

average mutual information can be found.

$$\mathbb{E}\{I(\mathbf{r}; \mathbf{x})\} \approx (2L+1) \cdot \log_2 \left(\frac{E}{(2L+1) \cdot N_0} \right) + \mathbb{E} \left\{ \sum_{l=1}^{2L+1} \log_2 \left((2L+1) \sigma_l^2 \right) \right\} \quad (17)$$

Note that $\mathbb{E}\{(2L+1)\sigma_l^2\} = 1$. Let us assume rich scattering and that the Fourier components of the antenna pattern are equally strong. Then we can roughly express the average mutual information as:

$$\mathbb{E}\{I(\mathbf{r}; \mathbf{x})\} \approx (2L+1) \cdot \log_2 \left(\frac{E}{(2L+1) \cdot N_0} \right) \quad (18)$$

Let us see what the spatial multiplexing gain of this scheme is. The spatial multiplexing gain can be defined as the ratio of the mutual information for the rotating antenna and the mutual information for a Multiple-Input-Single-Output (MISO) system. The spatial multiplexing gain becomes then:

$$\frac{(2L+1) \log_2 \left(\frac{E}{(2L+1) \cdot N_0} \right)}{\log_2 \left(\frac{E}{N_0} \right)} = (2L+1) \left(1 - \frac{\log_2(2L+1)}{\log_2 \left(\frac{E}{N_0} \right)} \right) \quad (19)$$

where $\log_2 \left(\frac{E}{N_0} \right)$ represents the average mutual information for a MISO-system. As we see from the equation, we do not get a multiplexing gain equal to the number of frequency components of the antenna pattern. Since there is a decrease in the effective SNR the multiplexing gain is reduced. Note that the reduction of the multiplexing gain vanishes for high SNR, although only logarithmically.

So far we have only considered the SNR that results from AWGN. If there are signals transmitting in adjacent frequency bands, these signals will be expanded in bandwidth too. The result will be that the frequency bandwidth of our signal of interest will overlap with the frequency bands of interfering signals. The received signal in the l -th sub-band may be written as:

$$r_l(t) = a_l \sum_{p=1}^P e^{j\phi_p l} s_p(t) + \sum_{i \neq 0} a_{l-i} \sum_{p=1}^P e^{j(l-i)\beta_{p,i}} q_{p,i}(t) \quad (20)$$

where $q_{p,i}(t)$ is an adjacent channel interference signal originating from frequency band $f_c - \frac{\omega_i}{2\pi}$. The subscript p denotes that the signal is arriving at angle $\beta_{p,i}$. The signals $s_p(t)$, $p = 1 \dots P$ are our desired signals. The effect that this interference has on our receiver depends on the nature of the interferers. In that respect we distinguish between two cases, operation in licensed and unlicensed bands. For operation in unlicensed bands the co-channel interference power might be comparable to the adjacent channel interference power. Therefore (19) can be a rough estimate of the performance of our system in unlicensed operation. The assumption made in this case is that the interference behaves as AWGN. For operation in licensed bands, signals that are transmitting in adjacent bands are expected to have higher power than co-channel interference. For this case it is unclear whether we can gain something from the rotating antenna system compared to MISO.

V. SAMPLING ISSUES

Until now we have not gone deep into the sampling issues of the antenna pattern. Section II dealt with a continuous rotating antenna, while Section III presented simulations when sampling the antenna pattern at discrete angles. This section will describe mathematically the sampling of the antenna pattern. Let us assume that the antenna pattern is sampled every T_c seconds, then we obtain

$$g_p(t) = \sum_{n=-\infty}^{\infty} a(\omega t + \phi_p) \delta(t - nT_c) \quad (21)$$

However this function consist of Dirac pulses, but in reality the antenna pattern function should hold a constant value for T_c seconds before it changes value. This can be obtained by folding $g_p(t)$ with a rectangular pulse $p(t)$. The rectangular pulse should have the duration of T_c seconds. Let us now define the sampled antenna pattern function as

$$\begin{aligned} a_{s,p}(t) &= g_p(t) * p(t) \\ &= \sum_{n=-\infty}^{\infty} \int_{\tau=-\infty}^{\infty} p(\tau) a(\omega(t-\tau) + \phi_p) \cdot \delta(t - nT_c - \tau) d\tau \\ &= \sum_{n=-\infty}^{\infty} p(t - nT_c) a(\omega nT_c + \phi_p) \end{aligned} \quad (22)$$

More insight is obtained by viewing this operation in the frequency domain. We note that a folding operation in the time domain is equivalent to multiplication in the frequency domain.

$$g_p(t) * p(t) \Leftrightarrow G_p(\Omega) \cdot P(\Omega) \quad (23)$$

In order to express $G_p(\Omega)$ we first need to find the spectrum of the continuous antenna pattern function $a(\omega t + \phi_p)$:

$$A_p(\Omega) = \mathcal{F}\{a(\omega t + \phi_p)\} = \sum_{l=-L}^L a_l \delta(\Omega + l\omega) e^{jl\phi_p} \quad (24)$$

where $\mathcal{F}\{\cdot\}$ denotes the Fourier transform. $G_p(\Omega)$ will consist of spectral copies of $A_p(\Omega)$ due to sampling:

$$\begin{aligned} G_p(\Omega) &= \sum_{k=-\infty}^{\infty} A_p \left(\Omega + \frac{2\pi k}{T_c} \right) \\ &= \sum_{k=-\infty}^{\infty} \sum_{l=-L}^L a_l \delta \left(\Omega + l\omega + \frac{2\pi k}{T_c} \right) e^{jl\phi_p} \end{aligned} \quad (25)$$

The sampled antenna pattern will therefore be given by:

$$\begin{aligned} A_{s,p}(\Omega) &= \sqrt{T_c} \text{sinc} \left(\Omega \frac{T_c}{2\pi} \right) \cdot \\ &\sum_{k=-\infty}^{\infty} \sum_{l=-L}^L a_l \delta \left(\Omega + l\omega + \frac{2\pi k}{T_c} \right) e^{jl\phi_p} \end{aligned} \quad (26)$$

Equation (26) shows that the sampled antenna pattern function consists of weighted spectral copies. The weighting is done by the sinc function $P(\Omega)$, where $P(\Omega)$ is just the Fourier transform of $p(t)$ in (22). The separation between each spectral copy is $\frac{2\pi}{T_c}$, which means it is determined by the sampling interval. An example will better illustrate the sampling issues

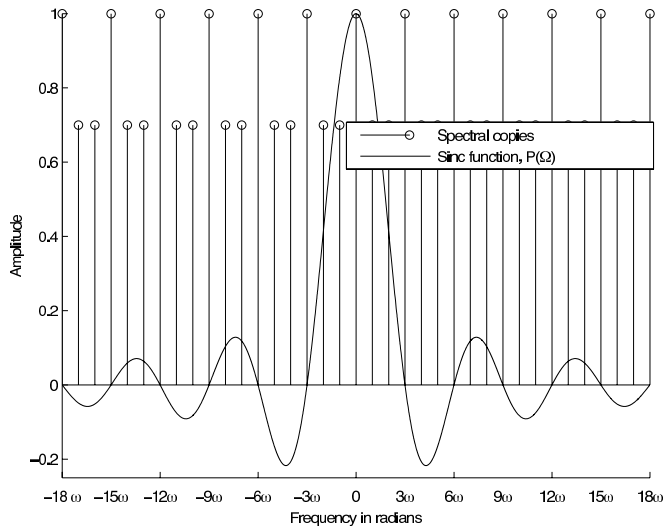


Fig. 7. Plots of $G_p(\Omega)$, the repeated spectral copies of the antenna pattern due to sampling, and $P(\Omega)$ which represents the hold operation. The continuously rotating antenna pattern consists of 3 frequency components. The antenna pattern is sampled at frequency 3ω , i.e. at the lowest sampling frequency that avoids aliasing.

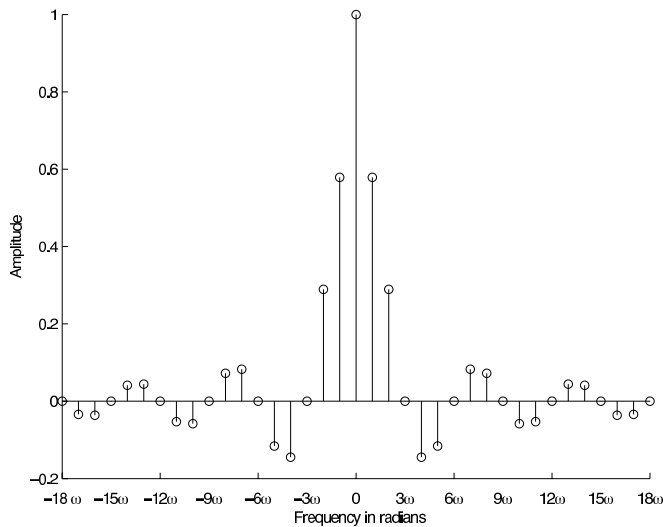


Fig. 8. The sampled antenna pattern function, which results from sampling at frequency 3ω . The corresponding continuously rotating pattern consists of 3 frequency components.

of the antenna pattern. Assume an antenna pattern function that has 3 harmonics. Fig. 7 shows $G_p(\Omega)$ and $P(\Omega)$ for the case when the antenna pattern function is sampled with frequency $\Omega_s = 3\omega$. The result of sampling the antenna pattern function is shown in Fig. 8. Note that a lower sampling frequency than 3ω gives overlap between the spectral copies and therefore results in aliasing. When comparing the number of harmonics of the continuously rotating antenna function $A_p(\Omega)$ with $A_{s,p}(\Omega)$, we see that the sampled antenna pattern function has several more harmonics than the continuously rotating antenna. This means that the spectrum of the received signal will be expanded even more in frequency with the sampled antenna pattern than with the continuous antenna pattern. This might lead us to the erroneous believe that the degrees of freedom for the sampled antenna pattern is even higher than when the antenna rotates continuously. We can see from (26) that the signal in the extra sub-bands have the same

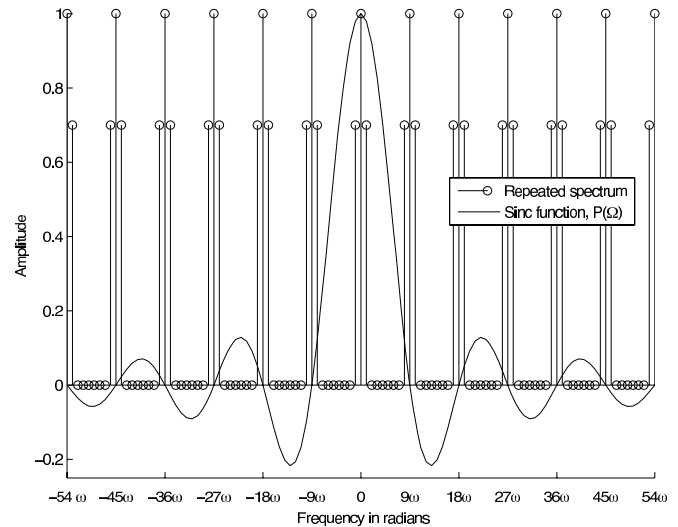


Fig. 9. Plots of $G_p(\Omega)$, the repeated spectral copies of the antenna pattern due to sampling, and $P(\Omega)$ which represents the hold operation. The continuously rotating antenna pattern consists of 3 frequency components. The antenna pattern is sampled at frequency 9ω , i.e. 3 times higher than the lowest sampling frequency that avoids aliasing.

linear combinations of the incoming waves as the original sub-bands. The same $e^{j\phi_{1l}}, \dots, e^{j\phi_{pl}}$ factors are used to weight the incoming waves. Therefore there will be no new information in these extra sub-bands.

This extra sub-bands can still be of use. Let us assume that there are no adjacent channel signals present, just AWGN. We have seen that the sampled rotating antenna spreads the signal bandwidth even more than the continuous rotating antenna. A wider signal bandwidth implies a higher noise bandwidth. However the sampled rotating antenna does not loose in terms of performance compared to the continuous rotating antenna. This holds under the assumption that the antenna pattern is sampled sufficiently. Consider a signal $r_l(t)$ in the l -th frequency sub-band and a spectral copy $r_{l+2L+1}(t)$ due to the discrete rotation in the $(l + 2L + 1)$ -th sub-band. From (26) we see that $r_{l+2L+1}(t)$ will be a scaled and phase-shifted version of $r_l(t)$. Let us assume that the SNR in the l -th and $(l + 2L + 1)$ -th sub-band is given by :

$$\text{SNR}_l = \frac{E_l}{N_0} \quad (27)$$

$$\text{SNR}_{l+2L+1} = \frac{E_l \cdot |a|^2}{N_0} \quad (28)$$

where the complex constant a indicates the scaling and phase-shift of the signal in the $(l + 2L + 1)$ -th sub-band. The energy of the signal of interest in l -th sub-band is given by E_l . By coherently combining the signal in the l -th and $(l + 2L + 1)$ -th sub-band we obtain a signal with SNR equal to $\frac{E_l \cdot (1 + |a|^2)}{N_0}$. If we coherently combine all the extra sub-bands due to discrete rotation we will achieve the same SNR as the continuous rotating antenna.

We proceed by finding a matrix expression similar to (5) for the received signal

$$\tilde{\mathbf{r}}(t) = \begin{bmatrix} \tilde{r}_{-K(2L+1)-L}(t) \\ \vdots \\ \tilde{r}_{+K(2L+1)+L}(t) \end{bmatrix} = \mathbf{PAVs}(t) + \mathbf{n} \quad (29)$$

$\tilde{\mathbf{r}}(t)$ is the received signal of the sampled rotating antenna. The dimension of $\tilde{\mathbf{r}}(t)$ is much higher than the dimension of \mathbf{r} , because the sampled rotating antenna spreads the signal even more. $2L + 1$ is the number of harmonics of the continuously rotating antenna, whereas K is an integer that describes the extra bandwidth expansion. From the matrix expression we see that the sampled antenna rotation is described by a multiplication with matrix \mathbf{P} with elements consisting of values from the sinc function. The structure of matrix \mathbf{P} will be

$$\underbrace{\begin{bmatrix} \vdots & \vdots & \vdots & \vdots & \vdots \\ P(-\omega L - \Omega_s) & & & & \\ \vdots & \ddots & & & \\ \vdots & & P(-\Omega_s) & & \\ & & & \ddots & \\ 0 & & & & P(\omega L - \Omega_s) \\ P(-\omega L) & 0 & & & \\ & & \ddots & \vdots & \\ & & & P(\omega \cdot 0) & \\ & & & & \ddots & \\ P(-\omega L + \Omega_s) & & 0 & & & P(\omega L) \\ \vdots & \ddots & & & & \\ \vdots & & P(\Omega_s) & & & \\ & & & \ddots & & \\ \vdots & \vdots & \vdots & \vdots & \vdots & \\ & & & & & P(\omega L + \Omega_s) \end{bmatrix}}_{2L+1} \quad (30)$$

If we assume that the number of rows of P grows large, i.e. $K \rightarrow \infty$, and we assume that the antenna pattern is sampled sufficiently, then we get

$$\mathbf{P}^H \mathbf{P} = \mathbf{I} \quad (31)$$

Note that sampling sufficiently means that the number of samples per rotation is not smaller than the number of frequency components of the antenna pattern. We now assume that the received signal can be written as

$$\tilde{\mathbf{r}}(t) = \mathbf{P} \mathbf{A} \mathbf{V} \mathbf{H} \mathbf{x}(t) + \mathbf{n} \quad (32)$$

where \mathbf{H} describes the propagation path from the transmitter antennas to a certain angular direction at the receiver, $\mathbf{x}(t)$ is the transmitted signal vector and $\mathbf{n}(t)$ is a AWGN vector. We proceed by finding an expression for mutual information for perfect channel knowledge at the receiver side and a spatially white transmitted signal

$$I(\mathbf{x}; \mathbf{r}) = \log_2 \det \left(\mathbf{I} + \frac{1}{N_0} \mathbf{P} \mathbf{A} \mathbf{V} \mathbf{H} \mathbf{H}^H \mathbf{V}^H \mathbf{A}^H \mathbf{P}^H \right) \quad (33)$$

$$= \log_2 \det \left(\mathbf{I} + \frac{1}{N_0} \mathbf{A} \mathbf{V} \mathbf{H} \mathbf{H}^H \mathbf{V}^H \mathbf{A}^H \mathbf{P}^H \mathbf{P} \right) \quad (34)$$

$$= \log_2 \det \left(\mathbf{I} + \frac{1}{N_0} \mathbf{A} \mathbf{V} \mathbf{H} \mathbf{H}^H \mathbf{V}^H \mathbf{A}^H \right) \quad (35)$$

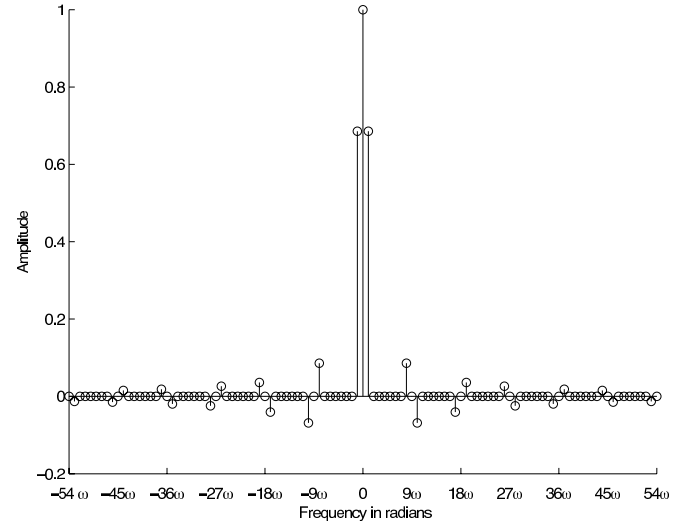


Fig. 10. The sampled antenna pattern function. The original antenna pattern consists of 3 frequency components. The antenna pattern is sampled at frequency 9ω .

(35) is identical to the expression for the mutual information for a continuously rotating antenna. This shows that mutual information becomes the same for the continuous rotating antenna and the sampled rotating antenna. From (33) to (34) the determinant principle is used. The principle says that the order of the matrices inside the determinant can be changed as long as the dimension of the identity matrix is also changed. The step from (34) to (35) assumes that we are including an infinite number of sub-bands, which means $\mathbf{P}^H \mathbf{P} = \mathbf{I}$. When \mathbf{P} contains only a finite number of sub-bands, then $\mathbf{P}^H \mathbf{P} = \mathbf{I}$ does not hold. The effect of this will be a somewhat larger eigenvalue spread of the matrix product $\mathbf{A} \mathbf{V} \mathbf{H} \mathbf{H}^H \mathbf{V}^H \mathbf{A}^H \mathbf{P}^H \mathbf{P}$, and therefore some decrease in mutual information.

A. Over-sampling

Since the receiver cannot, because of complexity, use too many subbands for reconstruction, an alternative might be to over-sample. Observe what happens if we over-sample the antenna pattern. Fig. 9 and Fig. 10 show the case when the sampling frequency is 9ω . This is three times higher than the number of frequency components of the continuously rotating antenna pattern. The effect of over-sampling is that the sampled antenna pattern function gets more similar to the continuously rotating antenna pattern function. This means that the power of the received signal is focused in a narrower frequency band, which is desirable. But there is also an unwanted effect by over-sampling which is caused by non-ideal switches. The more often we perform a switch the more often broadband impulse noise occurs. Since there is a trade-off between these two effects, there will be an optimum oversampling factor in practice.

B. Under-sampling

Under-sampling relates to sampling the wave-field with fewer samples per rotation than the number of frequency components of the antenna pattern. This case is more of

theoretical interest than practical, since we would of course take advantage of all the available degrees of freedom and not "loose" it by under-sampling. To illustrate what happens when we under-sample the wave-field, consider this example: Assume an antenna pattern with $2L + 1$ harmonics which is sampled by $2L$ samples per rotation. This would give spectral aliasing which is reflected in the \mathbf{P} matrix:

$$\underbrace{\begin{pmatrix} \vdots & \vdots & \vdots & \vdots & \vdots \\ P(-3\omega L) & \ddots & 0 & \dots & 0 \\ \vdots & & P(-2\omega L) & & \vdots \\ 0 & \dots & 0 & \ddots & 0 \\ P(-\omega L) & 0 & \vdots & 0 & P(-\omega L) \\ 0 & \ddots & 0 & 0 & 0 \\ \vdots & & P(\omega \cdot 0) & & \vdots \\ 0 & \dots & 0 & \ddots & 0 \\ P(\omega L) & 0 & \vdots & 0 & P(\omega L) \\ 0 & \ddots & 0 & 0 & 0 \\ \vdots & & P(2\omega L) & & \vdots \\ 0 & \dots & 0 & \ddots & 0 \\ P(3\omega L) & 0 & \dots & 0 & P(3\omega L) \\ \vdots & \vdots & \vdots & \vdots & \vdots \end{pmatrix}}_{2L+1} \quad (36)$$

When the wave-field was sampled sufficiently, there was only one element different from zero in each row. Under-sampling results in more than one element different from zero in each row. For the above case there are two elements that are different from zero. Note also that the two elements have the same value. The consequence of this is that the product $\mathbf{P}^H \mathbf{P}$ becomes a matrix which has two equal rows. This has the effect of losing one eigen-mode from the complete channel matrix and therefore one degree of freedom.

C. Adaptive rotation speed

The rotation of the antenna pattern expands the received signal bandwidth. The additional subbands that are created have a high chance of being occupied by other users. Therefore it would be advantageous to select a rotation speed that spreads our signal of interest into subbands that have small or ideally no interfering signals. If our antenna rotates at angular speed ω , the subbands will be spaced ω apart in frequency. If we choose n -fold rotation speed $n\omega$, then the subbands will be spaced $n\omega$ apart. The practical implementation of such an adaptive rotation scheme is simplest if $\frac{T}{T_c}$ is a prime number. Assume that we have 7 parasitic elements distributed evenly on a circle around the active receiver antenna. This configuration gives the possibility of 3 different rotation speeds. Let us number each of the parasitic element from 1 to 7. The 3 different rotation speeds are enabled by activating the parasitics in the

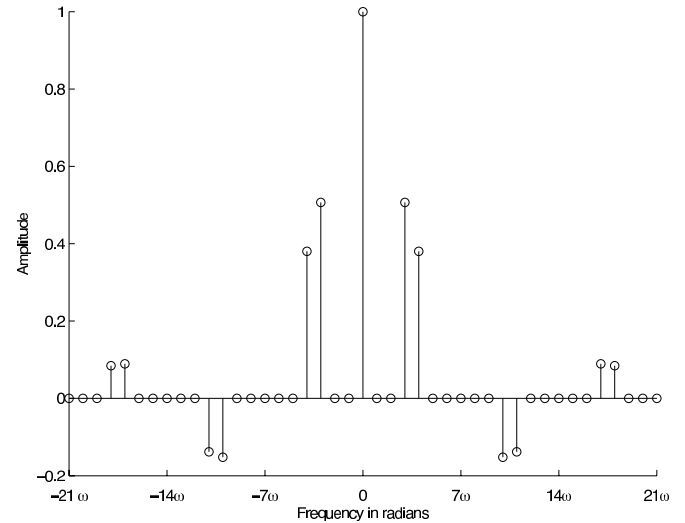


Fig. 11. Sampled antenna pattern obtained by rotation frequency 3ω and sampling frequency 7ω .

following order

$$\begin{array}{ll}
 \text{Basic speed} & 1 - 2 - 3 - 4 - 5 - 6 - 7 \\
 \text{Double speed} & 1 - 3 - 5 - 7 - 2 - 4 - 6 \\
 \text{Triple speed} & 1 - 4 - 7 - 3 - 6 - 2 - 5
 \end{array} \quad (37)$$

Note that each parasitic stays short-circuited for the same duration for each of these rotation speeds. The only difference between these rotation speeds is in which order the parasitics are short-circuited. Fig. 11 shows the frequency domain description of the sampled antenna pattern function for a triple rotation speed. It is assumed that the activation of 1 parasitic element gives an antenna pattern with 3 harmonics. Triple rotation speed, 3ω , gives a separation of 3ω between each harmonic of the continuously rotating antenna. A sampling frequency of 7ω , since we are using 7 parasitic elements, yields 7ω separation in frequency between each spectral copy. As a result of the triple rotation, the received signal is mainly modulated into frequency bins $f_c - 4\omega$, $f_c - 3\omega$, f_c , $f_c + 3\omega$, $f_c + 4\omega$, where f_c is the carrier frequency.

VI. IMPACT OF SCATTERING RICHNESS ON PERFORMANCE

From regular MIMO systems we know that a high amount of scattering is necessary to achieve high multiplexing gain. It is expected that the rotating antenna system will have the same dependency on the scattering richness as a regular MIMO system. In order to investigate this we perform simulations. We calculate mutual information as a function of angular spread. An angular spread of 45 degrees means that the scatterers are uniformly distributed within an angle of 45 degrees in the azimuth plane. Fig 12 shows mutual information for an increasing angular spread when a total of 100 scatterers are assumed. The simulations show that the mutual information increases with increasing angular spread. When the angular spread is 360 degrees the reactively loaded antenna achieves 21 bits/s/Hz. For an angular spread of 18 degrees the mutual information drops down to 8 bits/s/Hz, which means it drops by a factor of 2.5. Thus the rotating antenna depends on rich scattering in order to obtain high spectral efficiencies.

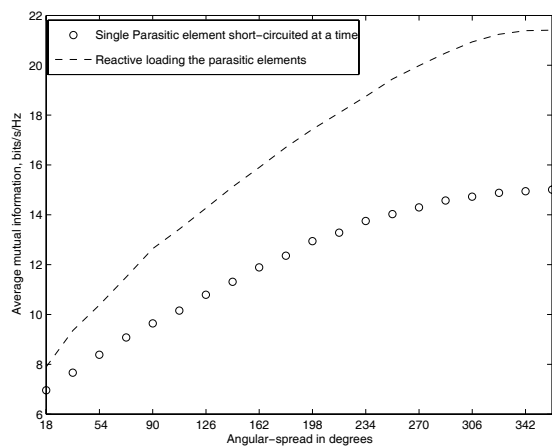


Fig. 12. Mutual information as a function of scattering angular spread. The scatterers are uniformly distributed within the angle.

VII. SUMMARY AND CONCLUSIONS

Traditional MIMO receivers use multiple antennas to receive different linear combinations of the transmitted signals. The disadvantage of using antenna arrays is the relatively large size the antenna system requires in order for the received signals to be sufficiently uncorrelated. We proposed a new kind of receiver that accesses the signal at a single antenna connector. By using parasitic elements to enable a rotating directive antenna beam, the received signal gets expanded in frequency. In each sub-band we receive different linear combinations of the transmitted signal which means an increased number of eigen-modes that can be used for communication. We have shown a few examples on how to practically implement this receiver and demonstrated the performance of such receivers in terms of ergodic mutual information. These practical implementations sample the wavefield at discrete angular directions. We found that reactively loading the parasitic elements resulted in 3.3 times higher ergodic mutual information than the MISO case for a SNR of 20 dB. Among the two ways of achieving directive antenna patterns, reactively loading the parasitic elements or parasitic elements with variable lengths, we conclude that the former showed a smaller frequency variation.

VIII. OPEN PROBLEMS

There are a number of open problems which need to be solved for this compact MIMO receiver. As mentioned earlier, the bandwidth expansion leads to adjacent channel signals being mixed up with our signal of interest. Therefore further research needs to look into appropriate equalizers for operation in licensed frequency bands. One possibility might be a "Viterbi-like" equalizer in the frequency domain. This paper did not consider the effects of the electronic switches attached to the parasitic elements. An evaluation of different switches, their non-ideal characteristics and design of optimum waveforms for the activation of these switches are important issues that need to be investigated. The small distance between the active receiver antenna and the parasitic elements leads to an antenna impedance which might be far from the standard

impedance of 50Ω . Therefore practical matching networks should be found, such that we get sufficient impedance match over a broad frequency band.

ACKNOWLEDGMENT

The authors would like to thank Jon Anders Aas for his assistance.

REFERENCES

- [1] E. Telatar, "Capacity of multi-antenna Gaussian channels," AT & T Bell laboratories, internal. tech. memo., June 1995.
- [2] G. J. Foschini and M. J. Gans, "On the limits of wireless communication in a fading environment when using multiple antennas," *Wireless Personal Communications*, vol. 6, pp. 311–335, Mar. 1998.
- [3] D. S. Shiu, G. J. Foschini, M. J. Gans, and J. M. Kahn, "Fading correlation and its effect on capacity of multielement antenna systems," *IEEE Trans. Commun.*, vol. 48, no. 3, pp. 502–513, Mar. 2000.
- [4] D. Gesbert, T. Ekman, and N. Christophersen, "Capacity limits of dense palm-sized MIMO arrays," in *Proc. IEEE GLOBECOM'02*, vol. 2, Nov. 2002, pp. 1187–1191.
- [5] T. Svantesson and A. Ranheim, "Mutual coupling effects on the capacity of multielement antenna systems," in *Proc. IEEE ICASP'01*, vol. 4, Salt Lake City, UT, May 2001, pp. 2485–2488.
- [6] R. Janaswamy, "Effect of element mutual coupling on the capacity of fixed length linear arrays," *IEEE Antennas Wireless Propagat. Lett.*, vol. 1, no. 2, pp. 157–160, 2002.
- [7] N. Chiurtu, B. Rimoldi, E. Telatar, and V. Pauli, "Impact of correlation and coupling on the capacity of MIMO systems," in *Proc. IEEE ISSPIT'03*, Dec. 2003, pp. 154–157.
- [8] J. B. Andersen and B. K. Lau, "On closely coupled dipoles in a random field," *IEEE Antennas Wireless Propagat. Lett.*, vol. 5, no. 1, pp. 73–75, Dec. 2006.
- [9] P. S. Kildal and K. Rosengren, "Electromagnetic analysis of effective and apparent diversity gain of two parallel dipoles," *IEEE Antennas Wireless Propagat. Lett.*, vol. 2, no. 1, pp. 9–13, 2003.
- [10] —, "Correlation and capacity of MIMO systems and mutual coupling, radiation efficiency, and diversity gain of their antennas: simulations and measurements in a reverberation chamber," *IEEE Commun. Mag.*, vol. 42, no. 12, pp. 104–112, Dec. 2004.
- [11] J. W. Wallace and M. A. Jensen, "Mutual coupling in MIMO wireless systems: a rigorous network theory analysis," *IEEE Trans. Antennas Propagat.*, vol. 3, no. 4, pp. 98–105, Jan. 2004.
- [12] —, "Termination-dependent diversity performance of coupled antennas: network theory analysis," *IEEE Trans. Commun.*, vol. 52, no. 3, pp. 1317–1325, July 2004.
- [13] M. L. Morris and M. A. Jensen, "Improved network analysis of coupled antenna diversity performance," *IEEE Trans. Wireless Commun.*, vol. 4, no. 4, pp. 1928–1934, July 2005.
- [14] A. S. Y. Poon, R. W. Brodersen, and D. N. C. Tse, "Degrees of freedom in multiple-antenna channels: a signal space approach," *IEEE Trans. Inform. Theory*, vol. 51, no. 2, pp. 523–536, Feb. 2005.
- [15] A. S. Y. Poon, D. N. C. Tse, and R. W. Brodersen, "Impact of scattering on the capacity, diversity, and propagation range of multiple-antenna channels," *IEEE Trans. Inform. Theory*, vol. 52, no. 3, pp. 1087–1100, Mar. 2006.
- [16] M. D. Migliore, "On the role of the number of degrees of freedom of the field in MIMO channels," *IEEE Trans. Antennas Propagat.*, vol. 54, no. 2, pp. 620–628, Feb. 2006.
- [17] M. Wennstrom and T. Svantesson, "An antenna solution for MIMO channels: using a switched parasitic antenna," in *Proc. IEEE PIMRC'01*, vol. 1, Sept. 2001, pp. 159–163.
- [18] A. Kalis and M. Carras, "Aerial entropy and capacity of an MEA EM source," in *Proc. 26th Symposium on Information Theory in the Benelux*, May 2005.
- [19] A. Kalis, A. G. Kanatas, M. Carras, and A. G. Constantinides, "On the performance of MIMO systems in the wavevector domain," in *Proc. 15th IST Mobile & Wireless Communications Summit*, Myconos, Greece, June 2006.
- [20] S. A. Zekavat and C. R. Nassar, "Smart antenna arrays with oscillating beam patterns: characterization of transmit diversity in semi-elliptic coverage," *IEEE Trans. Commun.*, vol. 50, no. 10, pp. 1549–1556, Oct. 2002.
- [21] R. Vaughan, "Switched parasitic elements for antenna diversity," *IEEE Trans. Antennas Propagat.*, vol. 47, no. 2, pp. 399–405, Feb. 1999.

- [22] K. Gyoda and T. Ohira, "Design of electronically steerable passive array radiator (espar) antennas," in *Proc. IEEE Antennas and Propagation Society International Symposium '03*, vol. 2, July 2000, pp. 922–925.
- [23] B. Schaer, K. Rambabu, J. Borneman, and R. Vahldieck, "Design of reactive parasitic elements in electronic beam steering arrays," *IEEE Trans. Antennas Propagat.*, vol. 53, no. 6, pp. 1998–2003, June 2005.
- [24] N. L. Scott, M. O. Leonard-Taylor, and R. G. Vaughan, "Diversity gain from a single-port adaptive antenna using switched parasitic elements illustrated with a wire and monopole prototype," *IEEE Trans. Antennas Propagat.*, vol. 47, no. 6, pp. 1066–1070, June 1999.
- [25] Y. Nakane, T. Noguchi, and Y. Kuwahara, "Trial model of adaptive antenna equipped with switched loads on parasitic elements," *IEEE Trans. Antennas Propagat.*, vol. 53, no. 10, pp. 3398–3402, Oct. 2005.
- [26] B. M. Kolundž, J. S. Ognjanovec, and T. K. Sarkar, *WIPL-D Electromagnetic Modeling of Composite Metallic and Dielectric Structures*. Boston, MA: Artech House, 2000.
- [27] R. R. Müller, "A random matrix model for communication via antenna arrays," *IEEE Trans. Inform. Theory*, vol. 48, no. 9, pp. 2495–2506, Sept. 2002.
- [28] M. Carras, A. Kalis, and A. G. Constantinides, "Improving the frequency characteristics of electronically steerable passive array radiator antennas," in *Proc. IEEE ISWCS'04*, Sept. 2004, pp. 130–134.
- [29] (1999, Oct.) Fast switching PIN diodes. Application note 929. Hewlett Packard. [Online]. Available: <http://www.home.agilent.com/agilent/home.jsp>
- [30] D. V. Thiel and S. Smith, *Switched Parasitic Antennas for Cellular Communications*. Boston, MA: Artech House, 2002.
- [31] R. F. Harrington, "Reactively controlled directive arrays," *IEEE Trans. Antennas Propagat.*, vol. 26, no. 3, pp. 390–395, May 1978.
- [32] D. Esser and H. Chaloupka, "Reactively reconfigurable two-port antennas for spatial techniques," in *Proc. 2006 Int. ITG/IEEE Workshop on Smart Antennas*, vol. 1, Günzburg, Germany, Mar. 2006.
- [33] B. K. Lau, J. B. Andersen, and A. F. Molisch, "Impact of matching network on bandwidth of compact antenna arrays," *IEEE Trans. Antennas Propagat.*, vol. 54, no. 11, pp. 3225–3238, Nov. 2006.
- [34] R. C. Hansen, "Fundamental limits in antennas," *Proc. IEEE*, vol. 69, no. 2, pp. 170–182, 1981.
- [35] V. Veremy, "Superdirective antennas with passive reflectors," *IEEE Trans. Antennas Propagat.*, vol. 37, no. 2, pp. 16–27, Apr. 1995.
- [36] M. L. Morris, M. A. Jensen, and J. W. Wallace, "Superdirectivity in MIMO systems," *IEEE Trans. Antennas Propagat.*, vol. 53, no. 9, pp. 2850–2857, Sept. 2005.
- [37] C. A. Balanis, *Antenna Theory: Analysis and Design*. John Wiley & Sons, Inc., 1997.



Robert Bains was born in Trondheim, Norway, 1978. He received the M.S degree and Ph.D. degree in electrical engineering at the Norwegian University of Science and Technology (NTNU) in 2003 and 2008, respectively.



Ralf R. Müller (S'96M'03SM'05) was born in Schwabach, Germany, 1970. He received the Dipl.-Ing. and Dr.-Ing. degree with distinction from University of Erlangen-Nuremberg in 1996 and 1999, resp. From 2000 to 2004, he was with Vienna Telecommunications Research Center (ftw.) in Vienna, Austria where he was head of the strategic wireless research division. Since 2005 he has been a full professor at the Department of Electronics and Telecommunications at the Norwegian University of Science and Technology in Trondheim, Norway. He

held visiting appointments at Princeton University, U.S.A., Institute Eurecom, France, the University of Melbourne, Australia, Babeş-Bolyai University in Cluj-Napoca, Romania, the University of Oulu, Finland, and the National University of Singapore. He also taught as an adjunct professor at Vienna University of Technology from 2001 to 2004. Dr Müller received the Johann Phillip Reis Award (jointly with R. Fischer) in 2005 and the Leonard G. Abraham Prize (jointly with S. Verdú) in 2002. He was independently presented awards by the Vodafone Foundation for Mobile Communications and the German Information Technology Society (ITG) for his doctorate thesis in 2000. Moreover, he received the ITG award in 2003. Dr Müller served from 2003 to 2006 as an associate editor for the IEEE TRANSACTIONS ON INFORMATION THEORY.